Z. Phys. A – Hadrons and Nuclei 341, 315–318 (1992)

Zeitschrift für Physik A Hadrons and Nuclei

Elastic scattering of 86 MeV ^{9}Li and 55 MeV ^{6}He on ^{208}Pb

N.K. Skobelev, S.M. Lukyanov, Yu.E. Penionzhkevich, S.P. Tretyakova, C. Borcea *, V.E. Zhuchko, V.A. Gorshkov, K.O. Terenetsky, V.P. Verbitsky**, and Yu.A. Pozdnyakov****

Laboratory of Nuclear Reactions, Joint Institute for Nuclear Research, Dubna, USSR

Received March 12, 1991; revised version August 5, 1991

The cross sections of elastically scattered ^{9}Li and ^{6}He on ^{208}Pb were measured. The scattered particles were detected by an annular CR-39 solid state nuclear track detector and the monitoring was done with a triple telescope of silicon detectors. The classical and optical model analyses of the measured elastic cross sections have been carried out. It was shown that the peripheral ^{9}Li interaction region has a rather high transparency. Strong dynamical polarization of ^{9}Li ions in the process of scattering is suggested.

PACS: 25.70.+Z; 25.70.+Cd

1. Introduction

The rapid development in the field of secondary beams offers a unique possibility to make spectroscopic studies of nuclei far from stability [1]. Up to now, one of the main goals of the secondary beam experiments was to measure the interaction cross sections at energies of few hundred MeV/A and hence to deduce the strong absorption radii of the light neutron rich nuclei [2, 3]. However, one has to remark that data on reaction cross sections are rather insensitive to the details of nucleon distribution in the peripheral region and to the interaction potential between the colliding ions [4].

For energies above the Coulomb barrier, a classical method of analysis [5] was employed for the elastic scattering data. According to this approach, particles moving on Coulomb trajectories may undergo a nuclear interaction and deviate from the initial ones. By studying the dependence of the experimental elastic scattering data on the distance of closest approach

$$D=(\eta/k)|1+1/\sin(\theta_{cm}/2)|, \quad (1)$$

where η is the Coulomb parameter, k is the wave number and θ_{cm} is the c.m. scattering angle, one may determine the interaction radius.

On the other hand, as the forward elastic scattering is mainly determined by the peripheral interaction of the colliding ions, a semimicroscopical optical model (OM) analysis can also be performed [6] starting from the nucleon distribution in the target and projectile.

2. Experiment

In the present work we report on elastic scattering of ^{6}He and ^{9}Li on ^{208}Pb. ^{6}He and ^{9}Li ions are emitted in the forward direction (9 msr) in the reaction ^{11}B (200 MeV) on Ta [7] and then are refocused and transported to the ^{208}Pb target by means of two 90° analyzing magnets and sextupoles used for the external beams of the U-400 cyclotron in Dubna. The Ta production target (500 mg/cm^2) was water cooled and fully stopped the incident ^{11}B beam.

The produced ^{6}He and ^{9}Li ions had a range that substantially exceeded the Ta target thickness. From the continuous energy spectrum of these ions, the two 90° dipoles selected the energies 57 MeV for ^{6}He and 86 MeV for ^{9}Li with a 2% accuracy. The scattering target was made of ^{208}Pb of 300 μg/cm^2 thickness.

The secondary beams passed through a collimating system (5 mm diameter) that defined an angular resolution of ±0.7°. The intensity of the focused ^{6}He and ^{9}Li beams on the scattering target amounted to $2\cdot10^3$ p/s, when the current of the primary ^{11}B beam was 1.5 μA. The scattered particles were detected by an annular CR-39 solid state nuclear track detector (SSNTD) and the control of the secondary ^{6}He and ^{9}Li beam composition was done by a triple telescope consisting of silicon detectors of 70, 150 and 2500 μm thickness, respectively, and placed in the central hole of the SSNTD [7]. After etching the plastic it was scanned under a microscope and the tracks of ^{6}He and ^{9}Li were identified by their diameters taking into account also the track inclinations with

* On leave from IFA Bucharest, Romania

** Institute for Nuclear Research, Kiev, USSR

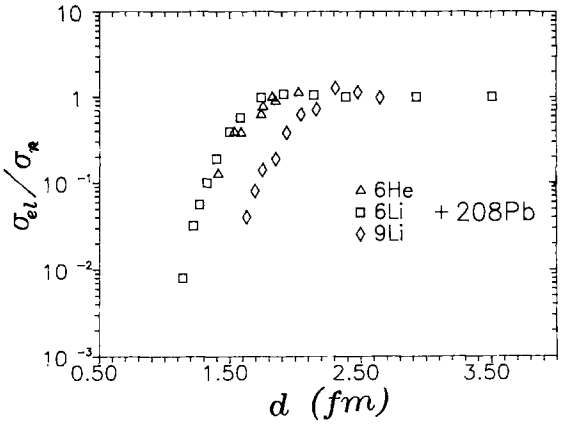

Fig. 1. The elastic to Rutherford cross section ratio as a function of the distance of closest approach parameter for ^{6}Li (51 MeV) [8], ^{6}He (55 MeV) and ^{9}Li (82 MeV) elastically scattered on ^{208}Pb

respect to the incident beam. The data on scattering of ^{6}He and ^{9}Li at different angles were obtained in one and the same experiment. The cross section ratio of the elastic scattered ions at small angles to the Rutherford scattering was normalized to unity.

The obtained elastic scattering differential cross sections, σ_{el}, divided by the Rutherford ones, σ_R, are given in Fig. 1 as a function of the distance of closest approach parameter

$$d = D/(A_t^{1/3} + A_p^{1/3}), \tag{2}$$

where A_t and A_p are the mass numbers of the target and projectile, respectively. In the same figure the data for the elastic scattering of ^{6}Li on ^{208}Pb, taken from [8], are also shown.

3. Data analysis

Obviously, the ratio σ_{el}/σ_R starts to deviate from unity at a value d_0 of the parameter d for which the nuclear interaction starts to manifest itself. The values of the d_0 extracted from the data are given in Table 1. One observes that d_0 for ^{6}Li and ^{6}He is practically the same but has a higher value for ^{9}Li. In order to understand this difference an optical model (OM) analysis of elastic scattering of ^{9}Li on ^{208}Pb has been performed. The results are given below.

3.1. Phenomenological optical model analysis

Here the six-parameter optical potential (OP) has been used

$$U(r) = V_c(r) + V_0 f_R(r) + iW_0 f_I(r), \tag{3}$$

Table 1. Distance of closest approach parameters

Reaction	C.M. Energy (MeV)	d_0(fm)
1. ^{6}He+^{208}Pb	55	1.65±0.05
2. ^{6}Li+^{208}Pb	51	1.65±0.03
3. ^{9}Li+^{208}Pb	82	2.1 ±0.05

Table 2. Optical potential parameters and χ^2/N values for the ^{9}Li +^{208}Pb system

Set	V_0 (MeV)	r_R (fm)	a_R (fm)	W_0 (MeV)	r_I (fm)	a_I (fm)	χ^2/N
1	−114.2	1.286	0.853	−9.4	1.739	0.809	–
2	−137.7	1.286	1.465	−9.4	1.739	0.809	19.3
3	−137.7	1.286	1.431	−5.8	1.739	1.693	7.1

where $V_c(r)$ is the uniform charged sphere Coulomb potential of radius $R_c = 1.3\,A_t^{1/3}$ fm. Form-factors $f_R(r)$ and $f_I(r)$ were chosen in the form

$$f_{R,I}(r) = \left[1 + exp\frac{r - r_{R,I}\,A_t^{1/3}}{a_{R,I}}\right]^{-1}. \tag{4}$$

Starting parameter values were adopted from the global ^{7}Li+^{208}Pb OP [9] (Set 1 of Table 2). At first, the parameters of the real part of the OP were fixed, while W_0 and a_I were fitted (r_I was fixed due to the Igo ambiguity [10]). It turned out that a satisfactory description of the data could not be achieved in such a fit.

Then we returned to the starting parameter values (Set 1 of Table 2) and fixed the parameters of the imaginary part of the OP, while V_0 and a_R were fitted (with fixed r_R). As a result a satisfactory description of the data was obtained. The parameters of the OP and the χ^2/N value are given in the second line of Table 2.

Finally, starting from Set 2 of Table 2, parameters V_0, W_0, a_R and a_I were varied simultaneously. Still better description of the elastic scattering differential cross section was obtained. The final set of the OP parameters and χ^2/N value are given in the third line of Table 2. The calculated differential cross section (solid curve) together with the experimental points are shown in Fig. 2.

As can be seen from Table 2 the diffuseness parameters a_R and a_I undergo the most strong variation during the fitting procedures. It should be noted that the value of a_R has decisive importance in the description of the considered data, while the a_I value determines only forward angle amplitude oscillations of the σ_{el}/σ_R. It is

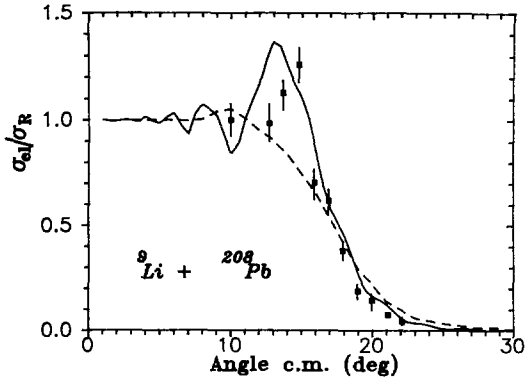

Fig. 2. The elastic to Rutherford cross section ratio for ^{9}Li+^{208}Pb as a function of c.m. scattering angle. The *solid curve* is the phenomenological OM fit to the data with Set 3 OP parameters of Table 2. *Dashed curve* – with the double folding model potential

worthwhile to note the surface transparency of the obtained OP. Really, we have $W/V=0.37$ at the strong absorption radius $D_{1/2}=13.9$ fm.

At the same time using the global OP [9] for the elastic scattering of ^{9}Li on ^{208}Pb at the same c.m. energy it is very easy to obtain $W/V=1.55$ at the strong absorption radius $D_{1/2}=12.0$ fm. It should be noted that the global OP for ^{7}Li was obtained in [9] from the analysis of the data set which includes only ^{7}Li on ^{208}Pb elastic scattering angular distribution at $E_{lab}=52$ MeV (Ecm $=50.3$ MeV). However, for the elastic scattering of ^{7}Li on ^{208}Pb at $E_{cm}=50.3$ MeV the global OP gives $W/V=1.57$ at $D_{1/2}=12.3$ fm. It is easy to see that close quantities are obtained for both energies. That is why we have used the OP from [9] for the calculation of the elastic scattering of ^{7}Li on ^{208}Pb at $E_{cm}=82.4$ MeV.

In order to understand the reason of the strong difference in the OP properties for ^{7}Li and ^{9}Li, we have undertaken the study of the peculiarities of the elastic scattering S-matrix in both cases and calculated the corresponding semi-classical deflection functions (DF). Results are presented in Fig. 3. The deflection functions

$$\theta(\lambda)=\theta_C(\lambda)+\theta_N(\lambda), \quad (5)$$
$$\lambda=l+1/2,$$

where l is the angular momentum, are shown in Fig. 3 by solid curves. The first addendum in (5)

$$\theta_C(\lambda)=2\arctan(\eta/\lambda) \quad (6)$$

is the Coulomb DF. In Fig. 3 $\theta_C(\lambda)$ are given by dashed curves. The second addendum in (5)

$$\theta_N(\lambda)=2\frac{d}{d\lambda}Re\delta(\lambda) \quad (7)$$

is the nuclear part of the DF while $\delta(\lambda)$ is the scattering phase.

Figure 3 shows a sharp difference between DF for ^{7}Li and ^{9}Li. The former DF only slightly differs in the region $l\geqq L_{1/2}$ ($L_{1/2}$ is the grazing angular momentum) from the Coulomb one. This means that in the ^{7}Li case, the action of the nuclear forces is revealed mainly in the ^{7}Li absorption, while refractive effects are negligible. In such a situation the elastic scattering differential cross section is determined mainly [11] by the superposition of the Coulomb and diffractive scattering.

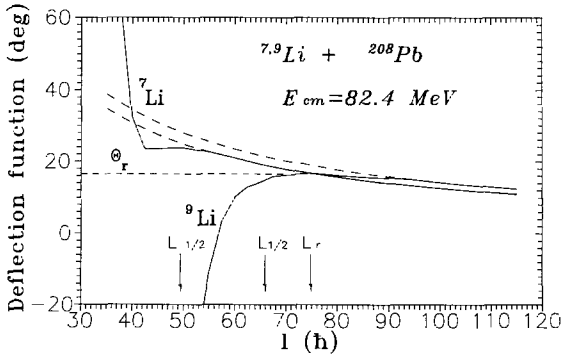

Fig. 3. Deflection functions for the ^{7,9}Li elastic scattering on ^{208}Pb at the same $E_{cm}=82.4$ MeV. *Solid curves* are total deflection functions, while *dashed* ones are the Coulomb deflection functions. $L_{1/2}$ – grazing angular momentum (left arrow – for ^{7}Li, right one – for ^{9}Li). L_r – Coulomb rainbow angular momentum for ^{9}Li

For ^{9}Li the picture of the elastic scattering changes abruptly. As can be seen from Fig. 3 in this case the DF has a well defined maximum $\theta_r=\theta(L_r)=16.9°$ at a rainbow angular momentum L_r. Besides, $L_{1/2}$ is less than L_r. All this means that the elastic scattering of ^{9}Li at least at angles $\theta<\theta_{1/4}$ ($\theta_{1/4}$ is that angle where the elastic scattering cross section is 1/4 of the Coulomb value) is determined by the refractive properties of the nuclei forces [11].

3.2. *Semimicroscopical OM analysis*

In the semimicroscopical OM analysis the optical potential

$$U(r)=V_c(r)+N_F\,V_F(r)+iW_0\,f_I(r) \quad (8)$$

was used. In (8) $V_F(r)$ is the double folded potential [6], N_F is its normalization constant, while the form-factor $f_I(r)$ is given by (4).

The proton density distribution for ^{208}Pb was obtained from the charge density distribution [12]. It was assumed that neutron and proton density distributions are the same. For ^{9}Li its matter density distribution taken from [13] was used. The effective nucleon-nucleon interaction was chosen in the $M3Y$ form [6].

The parameters N_F, W_0 and a_I were fitted. Usually this is enough for obtaining a good description of heavy ion elastic scattering data, if r_I is chosen properly (see, for example, [6]). But in our case it was impossible to obtain even a satisfactory fit (broken curve in Fig. 2). It means that the ^{9}Li on ^{208}Pb elastic scattering description demands on OP with a real part shape strongly deviating from a folding model potential one.

In conclusion let us return to Fig. 1. At the beginning of this section we pointed out that the elastic scattering differential cross section for ^{9}Li begins to deviate from the Coulomb one at a larger d_0 value compared with the ^{6}Li and ^{6}He cases. This happens, as can be seen from Fig. 1, at $d=d_0=2.1$ fm or at $D=d_0(A_t^{1/3}+A_p^{1/3})=16.8$ fm. Now let us turn to the DF for ^{9}Li presented in Fig. 3. It is easy to see that the DF just begins to deviate from the Coulomb one approximately at $l=L_0=90$ ħ. Supposing that the corresponding trajectory is a Coulomb one it is easy to find the distance of closest approach, $D=17.8$ fm. As can be seen, the so obtained distances are close to each other. This means that the peculiarities of the elastic scattering differential cross section of ^{9}Li on ^{208}Pb, presented in Fig. 1, are determined by the specific mechanism of elastic scattering in this case – viz. the Coulomb rainbow scattering.

4. Discussion and conclusions

OM analysis of the elastic scattering of ^{9}Li on ^{208}Pb at 86 MeV shows that surface transparent OP is neces-

sary for the description of the data. This is achieved by strengthening the real part of the OP in the vicinity of the strong absorption radius. However, this result was not confirmed by semimicroscopical folding model potential calculations. That is why one should assume that strengthening of the real part of the OP in the considered case is of dynamical nature.

In principle, a strong distortion of the folding model potential can be caused by coupling of the elastic scattering channel with the open reaction channels (^{9}Li break-up in the Coulomb and nuclear fields, inelastic scattering, nucleon transfers) as well as dynamical polarizability of ^{9}Li (coupling with closed reaction channels). Analogous effects for ^{208}Pb are probably strongly damped because it is a double magic nucleus. At the same time, it is well known that at energies above the Coulomb barrier Coulomb break-up [14], inelastic scattering and nucleon transfer reactions [15] contribute mainly to the imaginary component of the dynamic polarization potential. As far as the break-up of the incident particle during the nuclear interaction with the target nucleus is concerned, it makes $N_F < 1$ [16], while in our case we have obtained $N_F \cong 3$.

Thus one can conclude that the dynamical polarizability of ^{9}Li may be the most probable reason of the strong distortion of the double folded potential for the system $^9\text{Li} + ^{208}\text{Pb}$. It can manifest itself as an effective enlargement of the interaction radius. For the neutron rich light "compact" nuclei this assumption is not unreasonable.

Naturally, final conclusions cannot be made just now. For this, experimental verification of the present data should be made as well as new data for elastic and quasielastic scattering of ^{8}He, ^{8}Li and ^{9}Li in a wide energy range are necessary.

The authors are indebted to Professor Yu.Ts. Oganessian for his permanent interest in the present work.

References

1. Detraz, C., Vieira, D.J.: Ann. Rev. Nucl. Part. Sci. **39**, 407 (1989)
2. Tanihata, I., et al.: Phys. Lett. **160** B, 380 (1985)
3. Mittig, W., et al.: In: Proceedings of the First International Conference on Radioactive Nuclear Beams, Berkeley, USA, October 1989; Myers, W.D., et al. (ed.), p. 446. Singapore: World Scientific 1990
4. Bertulani, C.A., Hussein, M.S.: Phys. Rev. Lett. **64**, 1099 (1990)
5. Oganessian, Yu.Ts., et al.: Nucl. Phys. A **303**, 259 (1978)
6. Satchler, G.R., Love, W.G.: Phys. Rep. **55**, 183 (1979)
7. Skobelev, N.K., et al.: Izv. AN SSSR, Ser. Phys. **54**, 2218 (1990)
8. Chua, L.T. et al.: Nucl. Phys. A **273**, 243 (1976)
9. Cook, J.: Nucl. Phys. A **388**, 153 (1982)
10. Igo, G.: Phys. Rev. **115**, 1665 (1959)
11. Frahn, W.E.: In: Heavy-ion, high spin states and nuclear structure. vol. 1, p. 157, Vienna, IAEA 1975
12. Jager, C.W. De, Vries, H. De, Vries, C. De: At. Data Nucl. Data Tables **14**, 479 (1974)
13. Tosaka, Y., Suzuki, J.: Nucl. Phys. A **512**, 45 (1990)
14. Srivastava, D.K., Basu, D.N., Redel, H.: Nucl. Phys. A **485**, 221 (1988)
15. Pollarolo, G., Broglia, R.A., Winther, A.: Nucl. Phys. A **406**, 369 (1983)
16. Sakuragi, Yu.: Phys. Rev. C **35**, 2161 (1987)